

## Article

# Efficient Separation of Ultrafine Coal Assisted by Selective Adsorption of Polyvinylpyrrolidone

Yujie Mei <sup>1,2</sup>, Qiuyu Lin <sup>1,2</sup>, Changning Wu <sup>2,3,4</sup>, Wei Huang <sup>2,3,4</sup>, Daofan Cao <sup>5,6</sup> and Ke Liu <sup>2,3,4,\*</sup>

<sup>1</sup> School of Chemistry and Chemical Engineering, Harbin Institute of Technology, Harbin 150001, China; 11949014@mail.sustech.edu.cn (Y.M.); 11849610@mail.sustech.edu.cn (Q.L.)

<sup>2</sup> Department of Chemistry, Southern University of Science and Technology, Shenzhen 518055, China; wucn@sustech.edu.cn (C.W.); huangw8@sustech.edu.cn (W.H.)

<sup>3</sup> Shenzhen Engineering Research Center for Coal Comprehensive Utilization, School of Innovation and Entrepreneurship, Southern University of Science and Technology, Shenzhen 518055, China

<sup>4</sup> Clean Energy Institute, Academy for Advanced Interdisciplinary Studies, Southern University of Science and Technology, Shenzhen 518055, China

<sup>5</sup> Birmingham Centre for Energy Storage (BCES), University of Birmingham, Birmingham B15 2TT, UK; dxc816@student.bham.ac.uk

<sup>6</sup> School of Chemical Engineering, University of Birmingham, Birmingham B15 2TT, UK

\* Correspondence: liuk@sustech.edu.cn; Tel.: +86-0755-8801-0097

**Abstract:** The efficient separation of ultrafine coal is a challenging process due to the ultrafine particle size and gangue entrainment. In this study, a polymer, polyvinylpyrrolidone (PVP), was introduced as a regulator for ultrafine coal beneficiation. The addition of PVP improved the combustible recovery of clean coal and decreased the ash content. This effect was also presented by the selectivity index. The regulation mechanism of PVP was investigated using diverse methods. The adsorption tests performed demonstrated the adsorption amount of PVP on coal, kaolinite, and quartz, which were related to the increase in the separation efficiency. A zeta potential analyzer was employed to elucidate the effect of PVP on the electrical properties of ultrafine particles. The results revealed that the electrokinetic potential of mineral was sensitive to the varying PVP concentration. The particle size distribution was observed to value the influence of PVP on the particle behavior, which was tested by a laser particle size analyzer. X-ray photoelectron spectroscopy was used to investigate the surface elemental compositions of coal, kaolinite, and quartz, which were regulated by the adsorption of PVP. This research is beneficial to understanding the role of PVP as regulators and provides a basis for the efficient separation of ultrafine coal.

**Keywords:** polyvinylpyrrolidone; ultrafine coal; adsorption; separation efficiency



**Citation:** Mei, Y.; Lin, Q.; Wu, C.; Huang, W.; Cao, D.; Liu, K. Efficient Separation of Ultrafine Coal Assisted by Selective Adsorption of Polyvinylpyrrolidone. *Minerals* **2022**, *12*, 725. <https://doi.org/10.3390/min12060725>

Academic Editors: Liuyi Ren, Wencheng Xia, Wei Xiao, Siyuan Yang and Kevin Galvin

Received: 15 April 2022

Accepted: 2 June 2022

Published: 6 June 2022

**Publisher's Note:** MDPI stays neutral with regard to jurisdictional claims in published maps and institutional affiliations.



**Copyright:** © 2022 by the authors. Licensee MDPI, Basel, Switzerland. This article is an open access article distributed under the terms and conditions of the Creative Commons Attribution (CC BY) license (<https://creativecommons.org/licenses/by/4.0/>).

## 1. Introduction

As the most abundant fossil fuel in the world, coal accounts for over 50% of China's total energy consumption. Coal washing, which results in a large amount of slime, has put the spotlight on the utilization of coal cleaning technologies [1]. However, coal slime is difficult to recycle, and the majority of coal slime produced is classified as solid waste. Thus, the aim of coal slime recycling is not only save energy but also protect the environment [2]. Coal slime generated by coal washing plants usually has a high content of gangue minerals, with a fine or ultrafine particle size [3]. Fine coal are particles with particle sizes less than 0.5 mm while particles with diameters less than 0.1 mm are defined as ultrafine [4].

Froth flotation is a relatively effective method used to separate fine particles [5] and is widely used for fine coal separation in many countries, including China. However, the reprocessing of ultrafine coal by flotation is often not economically viable. The grain size is an important factor in flotation, especially for ultrafine particles, which need a longer processing time, higher energy, and more reagent consumption, to obtain a good separation performance [6]. Since hydrophobic coal particles tend to float on the water surface, partial

gangue particles can be embedded in coal, causing gangue entrainment. Meanwhile, the gap between coal and gangue narrows down at ultrafine grain sizes [7]. Attempts have thus been made to improve ultrafine coal flotation. Methods to enhance flotation can be divided into physical and physicochemical methods, such as changing the flow pattern of the air supply [4]; pre-conditioning coal slurry with microbubbles [8], nanobubbles [9], and high-voltage treatment [10]; carrier flotation [11]; selective oil agglomeration [12]; and the introduction of a mixed reagent system [13].

For the secondary recycling of carbonaceous resources from coal slime, the introduction of a flotation reagent has been considered as a research hotspot and an effective antidote to improve the separation efficiency. Traditional hydrocarbon oil collectors, such as diesel oil and kerosene, are widely used for coal flotation. However, oil consumption during coal slime separation is very high [14]. The adhesion of reagents on particles is a complicated process and is affected by the grain size, the type of additives used, and the pH of the solution [15,16]. It is difficult to obtain good adhesion or adsorption of non-polar oil collectors on ultrafine coal, wherein a limited efficiency is achieved due to the ultrafine grain size and particle–bubble attachment [17]. Due to the application of large machinery and the rapid dissociation rate of coal particles during modern coal processing, the high surface roughness and high ash content deteriorate the performance of ultrafine coal flotation [18]. Some surfactants have been proposed to improve the performance of coal recycling. Xia et al. used a cationic surfactant called dodecyl trimethyl ammonium bromide to enhance the adsorption of oil collectors on the coal surface, which improved the collection efficiency of dodecane limited by the oxygen functional groups on the coal surface [19]. Temperature also plays a key role in the adsorption of surfactants: Marsalek et al. found that the adsorption of cetyltrimethylammonium bromide on coal was influenced by temperature [20]. The introduction of surfactants plays a similar role in coal surface modification, adjusting the proportion of coal surface functional groups and reducing the effect of the coal surface roughness on the adhesion process [21]. It can be concluded that compound reagents contribute to an improved regulation performance in coal flotation. Numerous studies have demonstrated the superiority of compound agents, whereas polymer reagents have often been ignored. For fine particles, polymer reagents possess the advantages of a lower dosage and better adhesion efficiency. Polymer reagents are currently attracting increasing attention. Zou et al. reported that the introduction of a polymer, such as hydrophobically modified polyacrylamide, improved the combustible recovery of coal flotation [22]. Li et al. took advantage of the collaboration between nanobubbles and polyaluminum chloride to efficiently separate fine coal, with the nanobubbles promoting the flotation recovery while polyaluminum chloride inhibited entrainment by increasing the grain size [23]. Lv et al. synthesized a novel pH-sensitive flocculant and studied its effect on fine particles [24]. Studies exploring the impact of polymer reagents on fine coal separation are burgeoning. However, it is crucial to improve the floatability and selectivity of ultrafine coal by developing novel reagents.

As a novel polymer reagent rarely used in coal separation, polyvinylpyrrolidone (PVP) was adopted in this study. PVP has been adopted in the pharmaceutical and petroleum industries as an additive for separation, and acts as a carrier of synthetic materials. Palchoudhury et al. used PVP nanoparticles as a carrier to separate oil from wastewater and recycled petroleum wastewater [25]. Alabresm et al. investigated the synergistic effect of PVP nanoparticles and oil-degrading bacteria for the remediation of oil-water mixtures [26]. To date, only a few studies have explored the impact of PVP on ultrafine coal separation. PVP plays a key role in many separation scenarios. Through an experimental investigation, this study proves that PVP can facilitate the separation of ultrafine coal.

To understand how PVP facilitates ultrafine coal separation, laboratory flotation tests were conducted to observe the influence of PVP on the separation performance. A selectivity index (*SI*) was introduced to measure the results. Subsequently, an ultraviolet spectrophotometer (Uv-vis) was used for the adsorption test, wherein the purified minerals were used to test the adsorption selectivity of PVP on coal, kaolinite, and quartz. The

agglomeration behavior of the ultrafine particles with the introduction of PVP was investigated using a laser particle size analyzer (LPSA). The electrokinetic potential of the particles was measured using a zeta potential analyzer, and X-ray photoelectron spectroscopy (XPS) was employed to analyze the surface energy change of the particles influenced by PVP. We hope that the results of this study will prove beneficial in terms of understanding the role polymer reagents play in ultrafine coal separation.

## 2. Materials and Methods

### 2.1. Materials

The coal slime (ultrafine coal) and clean coal samples were procured from RecoTech Co., Ltd. (Tsingtao, China). Kaolinite and quartz were purchased from Beijing Mairuida Technology Co., Ltd. (Beijing, China). To understand the basic details of coal slime, we carried out proximate and elemental analyses (Table 1). We observed that the ash content of coal slime was 55%, and the ash content of clean coal was lower than 8%. The gross calorific value of clean coal was 24.02 MJ/kg, and its vitrinite reflectance was less than 0.5%. It could thus be classified as sub-bituminous coal according to ISO 11760. To identify the primary gangue mineral composition in coal slime, the ultrafine coal was scanned by X-ray diffraction (XRD, Rigaku Smart Lab, Tokyo, Japan). The results showed that the main gangue components were quartz and kaolinite (Figure 1). An LPSA (Beckman, LS 13320, Brea, CA, USA) was used for the particle size distribution analyses (Figure 2). The results showed that the mean size ( $D_{50}$ ) of coal slime was 23.73  $\mu\text{m}$ , with the size of 90% of the fine particles ( $D_{90}$ ) being 76.91  $\mu\text{m}$ , which was much lower than 0.1 mm. Thus, the coal slime was ultrafine coal. To further explore the adsorption and agglomeration properties of the ultrafine particles, clean coal, kaolinite, and quartz were also ground to the ultrafine grain size. Correspondingly, the size distribution of clean coal, quartz, and kaolinite is shown in Figure 3. The  $D_{50}$  of clean coal, quartz, and kaolinite is 24.11, 6.52, and 5.51  $\mu\text{m}$ , respectively.

**Table 1.** Proximate and elemental analyses of coal slime (ultrafine coal).

chemical results	Industrial Analysis/%				Elemental Analysis/%				
	$M_{ad}$	$A_{ad}$	$V_{daf}$	$FC_{daf}$	$C_{daf}$	$H_{daf}$	$N_{daf}$	$S_{daf}$	$O_{daf}^*$
	2.03	55.0	23.41	64.58	65.19	5.34	1.04	1.61	26.82

Note: M—moisture; A—ash; V—volatile; FC—fixed carbon; ad—air-dry basis; daf—air-dry ash free basis; \* by difference.

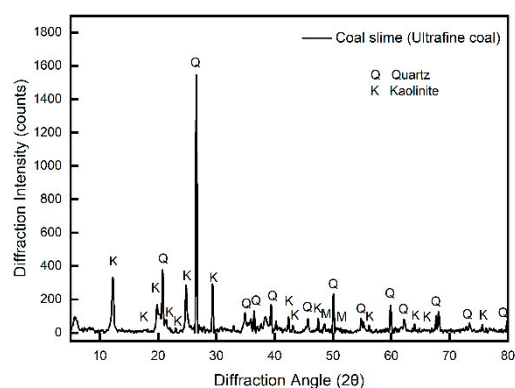


**Figure 1.** XRD result of coal slime (ultrafine coal).

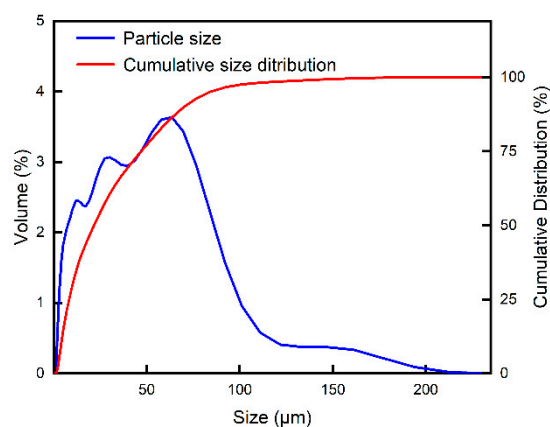


Figure 2. Size distribution of coal slime (ultrafine coal).

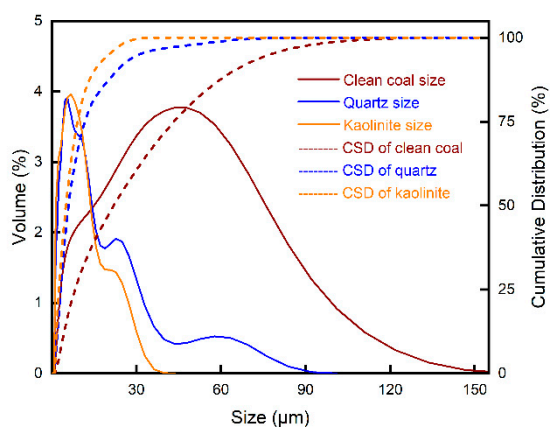


Figure 3. Size distribution of clean coal, quartz, and kaolinite.

All the reagents used in the experiments (purchased from Shanghai Macklin Biochemical Co., Ltd., Shanghai, China) are listed in Table 2. The solvent used in this study was deionized water (Milli-Q Integral 5, France), with a resistivity of less than 18.2 MΩ cm.

Table 2. List of reagents.

Name	Purity	Molecule Weight	Abbreviation
dodecane	≥99%	170	DD
polyvinylpyrrolidone		27,000	PVP
2-octanol	≥99%	130	2-octanol

Polyvinylpyrrolidone ( $C_6H_9NO$ )<sub>n</sub> is a non-ionic polymer. The average molecule weight of PVP used in this paper was 27,000. Its partial macromolecular structure is shown in Figure 4.

## 2.2. Laboratory Flotation Test

The laboratory flotation tests of ultrafine coal were carried out in an XFD flotation cell purchased from Wuhan Exploration Machinery Co., Ltd. (Wuhan, China). The flotation cell volume was 1 L. In total, 80 g of coal slime and 800 mL of water were added to prepare the suspension (8 wt%). Dodecane (DD) was used as the collector, 2-octanol was used as the frother, and PVP (used as the regulator) was dispersed into the slurry before flotation. The PVP solution was introduced at several concentrations (1, 3, 6, 10, 15 mg/L) to test its effect on recovery. PVP was added for 1 min of preset mixing, then DD (0.064 mg/mL) and 2-octanol (0.04 mg/mL) were added to the flotation cell. For all the flotation tests, the stirring speed of the agitator was maintained at 1500 rpm and the air supply rate was

set to 0.15 m<sup>3</sup>/h. The flotation cell was filled to the level of the standard waterline with tap water (pH = 6.8). All the tests were conducted at 25 °C. The separation products were collected, filtered, and dried in a ventilated drying oven at 95 °C. Proximate analysis was then conducted to clear the ash content of the samples.

The recovery of flotation was calculated using Equation (1):

$$R = \frac{M_f}{M_t} \cdot 100\% \quad (1)$$

where  $M_f$  is the dried weight of combustible matter (mainly coal) or ash (mainly quartz and kaolinite),  $M_t$  is the weight of the total feedstock of flotation cell (weight of coal slime), and  $R$  is the flotation recovery.

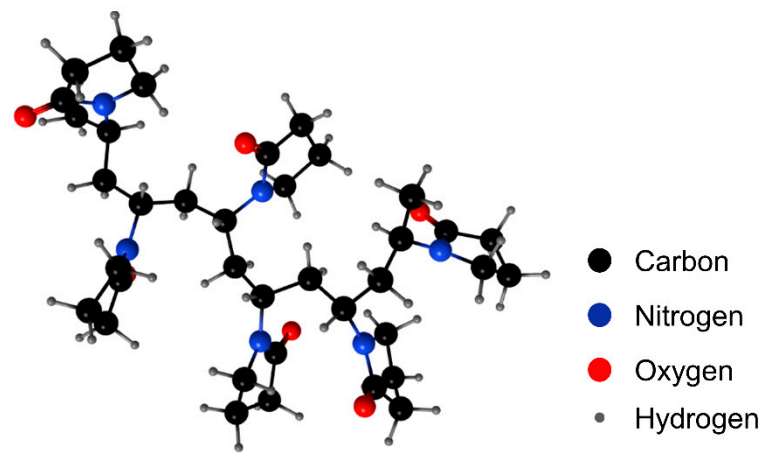


**Figure 4.** Partial macromolecular structure of PVP [27].

The flotation recovery can reflect the yield of clean coal. However, some further explanation is required for the separation selectivity. Thus, we first calculated the flotation rate. Some scholars have assumed that the flotation process can be described as a first-order reaction [28]. The first-order dynamics equation assumes that all matter floats at the same rate. In fact, due to differences in the grain size and mineral species, particles should have different flotation parameters. This study used Kelsall's model to calculate the flotation rate as shown in Equation (2) [27]:

$$R = R_{max} - [R_{fast} \cdot e^{-k_f t} + (R_{max} - R_{fast})] \cdot e^{-k_s t} \quad (2)$$

where  $R_{max}$  is the maximum theoretical recovery,  $R_{fast}$  is the maximum recovery of the fast floating fraction, and  $k_f$  and  $k_s$  are the rate constant of the fast float and slow float components, respectively. For practical purposes, flotation separation is often carried out using multi-stage circulation. The fast-float stage often plays the reference role for the particle cycling duration time in the flotation circuit while the slow stage is not worth saving. Thus, we mainly analyzed the parameters of the fast stage, which was more reasonable. Therefore, the rapid stage is usually more important, where  $R_{max}$  and  $k_f$  determine the efficiency. The solver tool in Excel was used for mathematical analysis of the fitting process, and the constraints for the parameters were added ( $R_{fast} \leq 100$ ,  $R_{fast} > R_{slow}$ ,  $k_f > k_s$ ). The rate function was set such that the operation represented the true physical process with the fast and slow stage. The modified rate constant ( $K_m$ , min<sup>-1</sup>) was introduced to value the response of different components as shown in Equation (3) [29]:

$$K_m = \frac{R_{max} \cdot k_f}{100} \quad (3)$$

We used the SSQ function to fit the results. The formula is Equation (4):

$$SSQ = \sum (R - \check{R})^2 \quad (4)$$

where  $R$  is the real recovery and  $\check{R}$  is the fitted value.

Finally, we introduce the selectivity index ( $SI$ ) to compare the flotation selectivity of serial tests. The  $SI$  was calculated using Equation (5) [30]:

$$SI\left(\frac{\text{combustible}}{\text{ash}}\right) = \frac{K_{m,com}}{K_{m,ash}} \quad (5)$$

where  $K_{m,com}$  and  $K_{m,ash}$  represent the modified rate constants of the combustible matter (mainly coal) and ash materials, respectively.

### 2.3. Adsorption Amount and Equilibrium Test

This study employed Uv-vis (UV-2600, Shimadzu, Japan) to test the adsorption characteristics of PVP. Before conducting the test, PVP was prepared as solutions with different concentrations (1, 3, 6, 10, 15, and 30 mg/L). Subsequently, 4 g of clean coal, quartz, and kaolinite were dispersed in 50 mL of PVP solution (8 wt%). The PVP solutions with a concentration of 6 mg/L were used to analyze the rate of adsorption. Pure PVP solutions without the solid samples were first scanned from 150–500 nm using Uv-vis to achieve the maximum absorbance value. The value of the peaks was consistently located at 194 nm. At the same time, the absorbance of PVP solutions with different concentrations was recorded to draw the calibration curve. Thereafter, the clean coal, kaolinite, and quartz particles were added to the PVP solutions. These mixtures were stirred at 500 rpm for 3 h to ensure sufficient adsorption of PVP on particles, which were then transferred into the centrifuge tube for a 10 min centrifugation at 10,000 rpm by High-Speed Centrifuge (Sorvall LYNX 6000, Thermo Fisher Scientific, Waltham, MA, USA). Then, the supernates were then extracted using a syringe and used for the Uv-vis test. The residual amount of PVP in the supernates was calibrated using the calibration curve, and the adsorption quality of PVP on the particles was deduced by subtraction. The adsorption amount of PVP on the particles was calculated by Equation (6):

$$A = [(c_0 - c_r + c_b) \cdot V \cdot 1000] / m \quad (6)$$

where  $A$  (mg/g) is the adsorption mass of PVP on the particles,  $c_0$  (mg/L) is the original concentration of the PVP solution used for the adsorption test,  $c_r$  (mg/L) is the residual concentration of PVP in the supernate after centrifugation,  $c_b$  is the dissolved matter of the solid particles in the supernate,  $V$  (mL) is the volume of the PVP solution, and  $m$  (g) is the corresponding net weight of the particles in the supernate. This method is called the subtraction method [31].

### 2.4. Zeta Potential Test

A zeta potential analyzer (Malvern Instruments, Malvern, Britain) was used to evaluate the properties of the ultrafine particles in terms of the surface charge and zeta potential value. Deionized water was used as a solvent, and 0.01 mol/L of KCL solution was prepared as the background electrolyte [32]. The pH during zeta potential measurement in this study was maintained at 6.8. PVP was completely dissolved in water and no flocs were observed. To understand the effects of the PVP concentration on coal, quartz, and kaolinite, we prepared eight different concentrations of the PVP solution (1, 2, 3, 6, 10, 15, 20, and 30 mg/L). Considering the increase in the self-aggregation and decrease in the water solubility of PVP with higher concentrations, concentrations greater than 30 mg/L were excluded from the test range. On the other hand, this study focused on the effects of the selective adsorption of PVP on ultrafine particles. Excessive PVP may induce supersaturated adsorption, thus reducing its adsorption selectivity and changing the role of

PVP in ultrafine coal separation. In total, 4 g of the solid sample (clean coal, kaolinite, and quartz) was added to 50 mL of the PVP solution and stirred for 3 h at 25 °C. Subsequently, 5 mL of the mixture was transferred into the centrifuge tube and centrifuged for 10 min at 10,000 rpm using the high-speed centrifuge (Thermo Fisher scientific, Sorvall LYNX 6000, Waltham, MA, USA). Thereafter, the supernate in the centrifuge tube was filtered and the filtrate was used for analysis. For each filtrate sample, tests were conducted several times with  $n$  repetition, and the standard error( $y$ ) of the zeta potential value was calculated by the STDEV function, given in Equation (7):

$$y = \sqrt{\frac{\sum(x - \bar{x})^2}{(n - 1)}} \times 100\% \quad (7)$$

where  $x$  is the test value and  $(\bar{x})$  is the average value for one point, and  $n$  is the number of test repetitions for one point. The value of  $y$  was set as the depth of the error bars and used to analyze the validity of the data.

### 2.5. Particle Size Distribution Test

The LPSA was used to evaluate the flocculation behavior of the ultrafine particles. The test system worked well in the wet method. Regarding the optical parameter of the analysis system, the real part of the medium refractive index was set to 1.8, 1.6, and 1.5 for coal, kaolinite, and quartz, respectively. Deionized water was used for sample dispersion and circulation, and an 8 wt% ultrafine particle suspension with 6 mg/L PVP was stirred at a rotation speed of 500 r/min for 3 h. Afterward, the dispersed sample was injected into the test system of the LPSA with a syringe. Agitation and ultrasonic defoaming were continued during the measurement [27].

### 2.6. XPS Test

XPS was used for the elemental analysis of clean coal, kaolinite, and quartz. To prepare the test samples with the PVP treatment, 4 g of clean coal, kaolinite, and quartz were added to 50 mL of PVP solution and stirred for 3 h at 25 °C. Then, 5 mL of the mixture was centrifuged and dried. To detect the surface changes, XPS was performed at 25 °C (ULVAC PHI 5000 VersaProbe III, Chigasaki, Japan). From a monochromatic X-ray source, the Al K $\alpha$  radiation ( $h\nu = 1486.6$  eV) and a light spot size of 200  $\mu\text{m}$  were set [33]. The spectra were recorded and stored at the pass energy of 26 eV in steps of 0.05 eV.

## 3. Results and Discussion

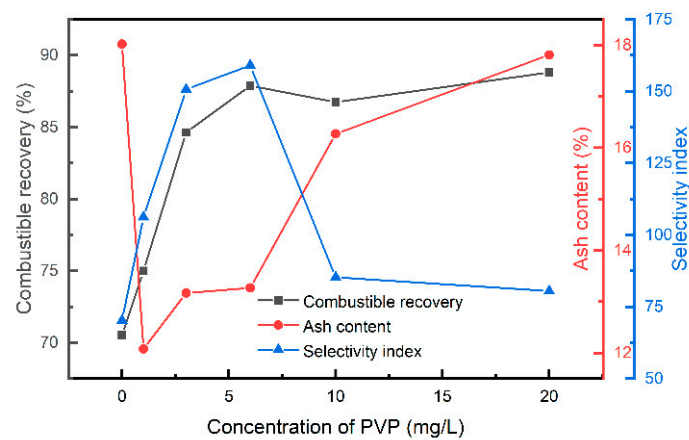
### 3.1. Laboratory Flotation

The mass recovery and flotation rate are used to evaluate flotation performance. We set up a series of flotation tests with different PVP concentrations and collected their separation products to calculate the recovery and flotation rate parameters. The results (Table 3 and Figure 5) revealed a difference in the flotation performance induced by PVP. The recovery and kinetic parameters ( $R_{max}$ ,  $k_f$ , and  $K_m$ ) were calculated and fitted by Equations (1)–(5). As seen in Table 3, the results indicated an increase in the combustible recovery of froth products with the introduction of PVP. Low dosages of PVP can relieve the constraints for ultrafine coal flotation recovery and can prove beneficial for reducing the number of oil collectors and energy consumption. The increase in the flotation rate proved that PVP facilitated the flotation of ultrafine particles, which can be attributed to the regulating role of PVP in particle behavior [27]. Meanwhile, the change in the ash recovery in the froth products was more complicated. In the tests with 1, 3, and 6 mg/L of PVP, the ash content appeared to be lower than the value in the test without PVP (blank control group). This seems to suggest that a low dosage of PVP is more likely to increase the flotation of combustible matter compared to the ash component. However, the maximum ash recovery of the flotation test with 20 mg/L PVP tended to approach the results of the blank control group. This difference could be attributed to the adsorption characteristics of PVP. Excessive

PVP can lead to the heterogeneous coagulation of coal and gangue particles. The modified rate constant  $K_m$  takes both the maximum recovery and flotation rate into consideration, which is considered fair regarding process evaluation. The value of  $K_{m,com}$  increased with a higher PVP concentration; on the contrary,  $K_{m,ash}$  was reduced with a higher PVP addition. The increase in the flotation rate constant can be attributed to the enhancement in the collision probability between the particles and bubbles [29]. The role of the reagents in this process was mainly focused on the surface modification of particles [34]. The agglomeration and adsorption behavior also provide evidence for the regulating role of PVP later in this study. Notably, when PVP exceeded a reasonable amount, the increase in the combustible recovery and ash recovery occurred simultaneously. More ash components disseminated in the froth products, limiting the further increase in  $R_{max,com}$  and  $K_{m,com}$ . To describe the changes and measure the impact of PVP on the separation efficiency, we calculated the  $SI$  (Equation (5)) of the flotation tests, and plotted it against other flotation indexes.

**Table 3.** Flotation kinetic parameters ( $R_{max}$ ,  $k_f$ , and  $K_m$ ) with varying PVP concentrations.

PVP (mg/L)	Combustible Matter			Ash		
	$R_{max}$	$k_f$	$K_{m,com}$	$R_{max}$	$k_f$	$K_{m,ash}$
0	41.36	3.13	1.29	28.37	0.14	0.04
1	43.93	3.28	1.44	23.88	0.11	0.03
3	59.77	4.16	2.49	21.51	0.08	0.02
6	84.58	3.23	2.73	22.08	0.08	0.02
10	78.76	3.67	2.89	28.54	0.12	0.03
20	80.01	3.62	2.90	35.69	0.10	0.04



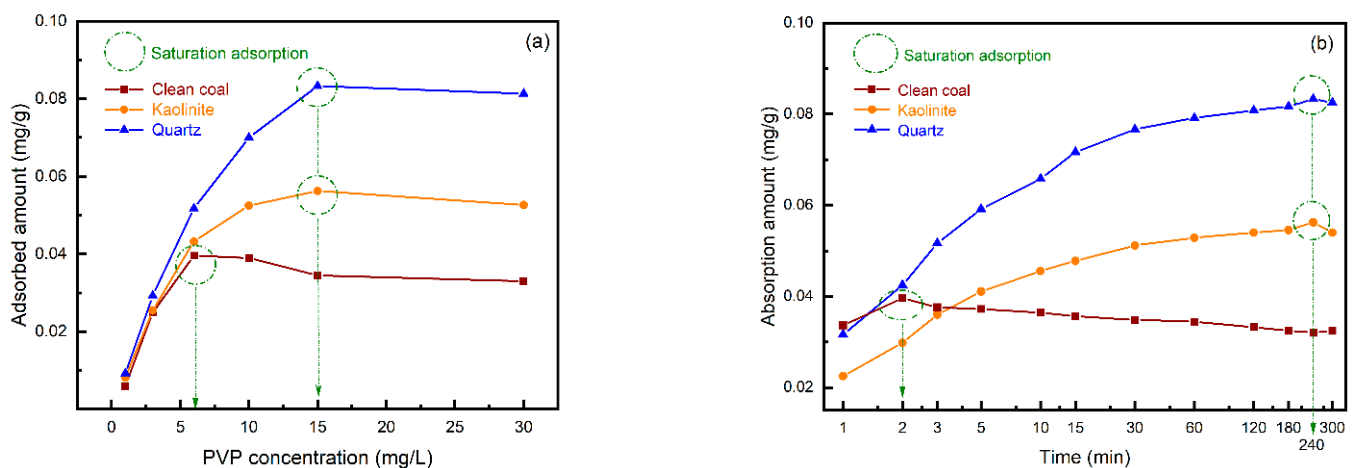
**Figure 5.** Combustible recovery (gray), ash content (red), and selectivity index (blue) of coal slime flotation with various concentrations of PVP.

Figure 5 shows the results of the combustible recovery and ash content of the froth products, and the calculated  $SI$  of various tests. As a blank control group, the tests without PVP yielded the highest ash content (18.02%) in the froth products, and the lowest combustible recovery (38.71%) and  $SI$  (70.22). Compared to the blank control group, the lowest ash content (12.08%) was achieved with 1 mg/L PVP. However, the combustible recovery and  $SI$  did not yield perfect results (70.53% and 106.21, respectively). The best  $SI$  (159.03) was obtained in the test conducted with 6 mg/L PVP; the ash content (13.17%) and combustible recovery (87.89%) were also great. The best maximum combustible recovery (88.81%) was obtained by the test performed with 20 mg/L PVP; however, the  $SI$  (85.26) was poor due to the increased entrainment of ash content (16.27%). Both the selectivity and recovery need to be considered when improving efficiency. Relatively good results were achieved with the 1 and 3 mg/L PVP concentrations. In general, particles tend to be coated by reagents, and the radius of particles and the length of the reagent play important roles

in flotation [35]. As a type of polymer, PVP has an advantage regarding the length of its molecular chain, which is effective in enhancing ultrafine particle flotation.

### 3.2. Adsorption Amount and Equilibrium

Uv-vis was used to test the adsorption capacity of PVP on the clean coal, kaolinite, and quartz particles. A hydration film typically exists on the surface of particles to prevent the collision or adhesion of particles, bubbles, or reagents. Effective adhesion is achieved only if the film is ruptured. Once stable adsorption is achieved, the amount of adsorption reflects the adsorption capacity. The results in Figure 6 prove that PVP adsorbed a less amount on coal than quartz and kaolinite regardless of the scale of the initial concentration of PVP (Figure 6a) or the equilibrium time (Figure 6b). In addition, the saturated adsorption amount of PVP on the particle surface, which is a critical parameter for determining the adsorption property, was closely related to the specific surface area of the particle. Although the saturated adsorption amount of PVP on kaolinite and quartz was greater than that on clean coal, the specific surface areas of kaolinite and quartz were much higher than on coal. It is worth mentioning that when the time increased, the adsorption of kaolinite and quartz increased correspondingly. At this moment, the initial concentration of PVP (6 mg/L) was more beneficial to the adsorption of PVP on coal. One explanation is that the adsorption strength of PVP could be stronger than that of gangue minerals, and the saturation adsorption amount was limited by the specific surface area of coal. However, the contact of the reagents with the particles in flotation was more complicated, wherein the adsorption efficiency was also influenced by the hydromechanical characteristics. Thus, the saturation adsorption of kaolinite and quartz was hardly achieved in the suspension adjustment process during flotation due to the process duration time. This could be the main reason for the improvement in the combustible recovery for low PVP dosages, and the increase in gangue entrainment can be attributed to the increase in PVP adsorption for high PVP dosages. Finally, it can be deduced that the enhancement in flotation was mainly related to the adsorption of PVP on the particles.



**Figure 6.** Adsorption amount of PVP on clean coal (wine), kaolinite (orange), and quartz (blue): (a) adsorption amount with an increase in the PVP concentration and (b) adsorption amount with an increase in time.

### 3.3. Zeta Potential

The measured zeta potential values of the clean coal, kaolinite, and quartz suspensions at different PVP concentrations are shown in Figure 7, where the error bars represent the standard deviation of the three replicate tests. As a widely used metric for analyzing the interaction of particles or macromolecules in the field of surface chemistry, the zeta potential explains changes in the electrostatic attraction or repulsion induced by PVP [36]. With 0.01 mol/L KCL, the mean value of the initial zeta potentials of kaolinite and quartz were

−37.68 and −42.41 mV, respectively, both of which were much higher than the −28.88 mV of clean coal. With an increase in the dosage of PVP, the zeta potential of clean coal fluctuated from −26.95 to −28.88 mV. The response was much weaker than the change noticed in gangue minerals. The zeta potential of kaolinite increased to −27.41 mV, whereas the zeta potential of quartz increased to −31.25 mV and then remained constant at the PVP concentration of 30 mg/L, which caused a strong electrostatic attraction between the gangue minerals. Kaolinite and quartz tended to agglomerate from the analysis of the homogeneous system. However, the zeta potential was measured under relatively ideal conditions of pure matter. In a real system of ultrafine coal separation, competitive adsorption of PVP can occur between different particles, and particle behavior is associated with the dosage of reagents. The ideal separation effect will only be maintained when the right range of reagent concentrations is used.

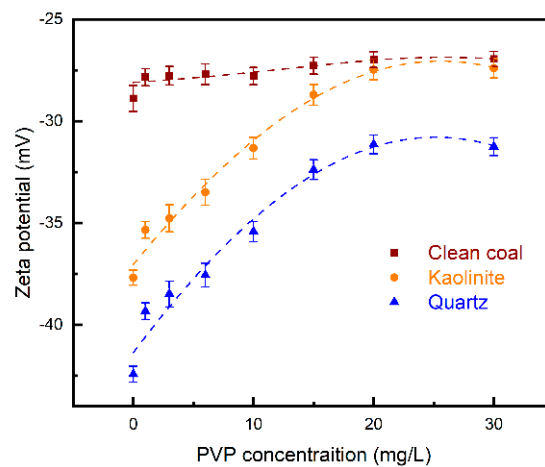


**Figure 7.** Zeta potentials of clean coal (wine), kaolinite (orange), and quartz (blue) with different PVP concentrations.

### 3.4. Particle Size Distribution

To explain the effect of PVP on the particle size distribution of clean coal, kaolinite, and quartz, we chose the PVP solution of 6 mg/L for the LPSA measurement, corresponding to the group that yielded the best *SI* results in the flotation test. The LPSA functions through light diffraction and scattering of particles. After eliminating the effect of the test environment and sample characteristics, an agglomeration tendency was noticed in all three types of particles with the assistance of PVP, as shown in Figure 8. The median size ( $D_{50}$ ) was often used to describe the feature size of a particle swarm. On the one hand, the  $D_{50}$  of the clean coal particles increased from 24.11 to 36.56  $\mu\text{m}$  after PVP adsorption, which was beneficial for combustible recovery. On the other hand, the  $D_{50}$  of the kaolinite and quartz particles was below 10  $\mu\text{m}$  (Figure 9). In comparison, the coal flocs tended to float upward after the adsorption of PVP, and the entrainment of kaolinite and quartz was depressed. This condition was consistent with the flotation behavior of ultrafine coal with the 6 mg/L PVP addition. Apart from  $D_{50}$ ,  $D_{90}$  represents the maximum diameters of 90% particles, which also presented growth. All the changes observed in the particle size distribution prove the effect of PVP adsorption on the particle behavior. By observing the adsorption amount of PVP on the surface of clean coal, kaolinite, and quartz, we formed the opinion that the addition of a low PVP dosage improves the selectivity during the flotation of ultrafine coal.

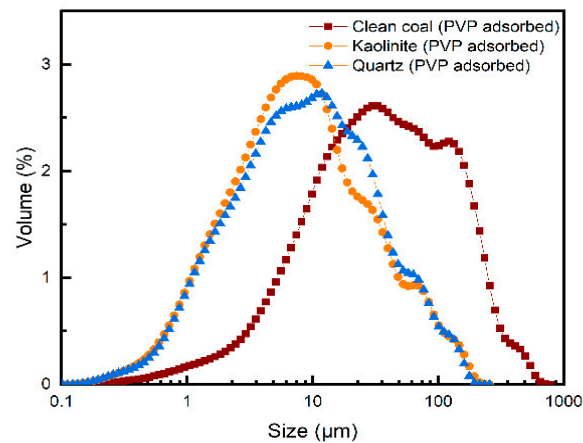


**Figure 8.** Size distribution of clean coal, quartz, and kaolinite (treated with 6 mg/L PVP).

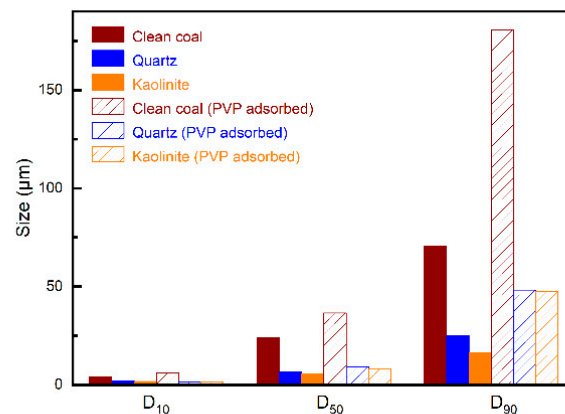


**Figure 9.** D10, D50, and D90 of clean coal, quartz, and kaolinite (treated with 6 mg/L PVP).

### 3.5. XPS

Figure 10 shows the wide energy spectrums of the clean coal, kaolinite, and quartz surfaces tested by XPS. On the one hand, the results (Figure 10a) illustrate that C (75.6%), O (19.0%), N (2.1%), Si (2.3%), and Al (1.0%) elements occupied the surface of clean coal. It was reported earlier that the proportion of N on the surface of PVP was higher than on coal [27]. Thus, the adsorption of PVP changed the elemental composition of the coal surface, mainly increasing the proportion of N from 2.1% to 3.6% (Figure 10b); on the other hand, the maximum peak of N1s also appeared on the kaolinite (Figure 10d) and quartz (Figure 10e) surfaces after PVP absorption, which can be attributed to the lactam group of PVP. The Si and Al content decreased with the absorption of PVP. The increase in the proportion of N observed on the surfaces of kaolinite and quartz was much lower than in coal [37,38]. In terms of the detection method, Uv-vis tends to analyze the adsorption amount of PVP while XPS tends to detect the surface adsorption form. Although the adsorption equilibrium amount of PVP in the gangue minerals was higher than in clean coal, XPS is a test that can be conducted for flat surfaces, excluding the influence of the grain size. In conclusion, PVP could be adsorbed on the coal, kaolinite, and quartz surfaces, resulting in better selectively in coal flotation.

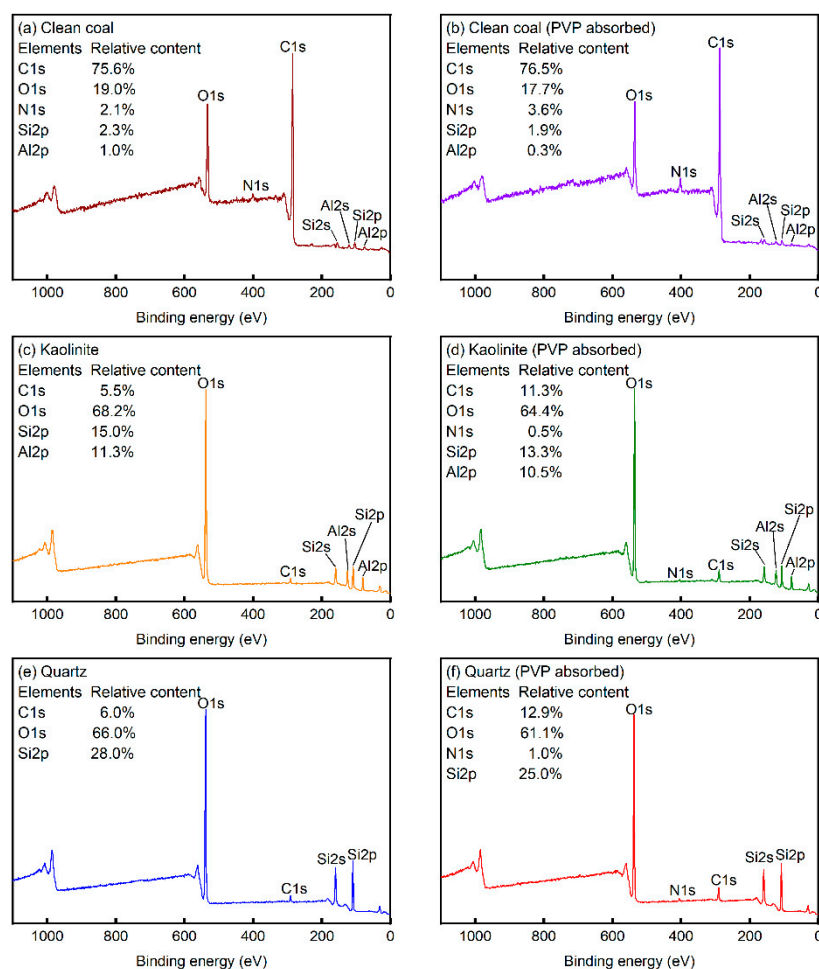


**Figure 10.** Changes in the wide energy spectrums of clean coal, kaolinite, and quartz tested by XPS: (a) clean coal, (b) clean coal with PVP treatment; (c) kaolinite, (d) kaolinite with PVP treatment; (e) quartz, (f) quartz with PVP treatment.

#### 4. Conclusions

This study investigated the influence of PVP on the efficient separation of ultrafine coal. The poor flotation performance of ultrafine coal can be attributed to the initial high ash content and ultrafine grain size. PVP was used to adjust the process before flotation and improve the flotation performance. The adsorption, zeta potential, particle size distribution, and an XPS test were investigated to illustrate the mechanism of the adjusting role played by PVP. The supporting analyses and the main conclusion are summarized as follows:

(a) PVP could be adsorbed on the surface of ultrafine coal. The adsorption amount of PVP was affected by the initial concentration of PVP and the adsorption time. The adsorption amount of PVP could be used to adjust the zeta potential of the particles and influence the attraction between them.

(b) The adsorption characteristics of PVP affected the flocculation of clean coal, kaolinite, and quartz, forcing more particles to float upward. The flotation rate and combustible recovery were significantly improved, and the *SI* value revealed an increase in the selectivity at low PVP concentrations.

(c) The separation process of ultrafine particles was highly sensitive to the polymer reagents. The addition of low concentrations of PVP led to an improvement in the separation efficiency, whereas excessive amounts of PVP were not conducive to separation.

(d) Polymer agents have wide application prospects and can be used to solve problems that are not proficient for the short-chain molecule. As polymers are easy to load or modify,

the influence of the long chain length of PVP can be further researched to achieve more efficient separation.

**Author Contributions:** Conceptualization, Y.M.; methodology, Y.M. and Q.L.; software, Y.M.; validation, C.W. and W.H.; formal analysis, W.H.; investigation, Y.M.; resources, D.C.; data curation, Q.L.; writing—original draft preparation, Y.M.; writing—review and editing, W.H.; visualization, Q.L.; supervision, K.L.; project administration, C.W. and K.L.; funding acquisition, K.L. All authors have read and agreed to the published version of the manuscript.

**Funding:** This research was funded by the project from the Shenzhen Development and Reform Commission (No. XMHT20190203001), Guangdong Innovative and Entrepreneurial Research Team Program (No. 2016ZT06N532) with Shenzhen Government Related Supporting Fund (No. KYT-DPT20181011104002), and RevTech-SUSTech Joint RMS Technology Development Project (OR2109006).

**Acknowledgments:** The authors acknowledge the assistance of SUSTech Core Research Facilities. The authors thanks for the help from Junguo, Li and Yumeng Chen during the research.

**Conflicts of Interest:** The authors declare no conflict of interest.

## References

1. Cai, Y.; Du, M.; Wang, S.; Liu, L. Determination of oxidation properties and flotation parameters of low-rank coal slimes. *Powder Technol.* **2019**, *353*, 20–26. [[CrossRef](#)]
2. Wang, G.; Bai, X.; Wu, C.; Li, W.; Liu, K.; Kiani, A. Recent advances in the beneficiation of ultrafine coal particles. *Fuel Process. Technol.* **2018**, *178*, 104–125. [[CrossRef](#)]
3. Zhao, X.; Tang, Y.; Zhao, B.; Wu, C.; Li, J.; Chu, C. Collecting behaviors of high internal phase (HIP) emulsion in flotation of ultrafine high-ash content coal slime. *Int. J. Coal Prep. Util.* **2021**, *41*. [[CrossRef](#)]
4. Wang, J.; Wang, L. Improving column flotation of oxidized or ultrafine coal particles by changing the flow pattern of air supply. *Miner. Eng.* **2018**, *124*, 98–102. [[CrossRef](#)]
5. Norori, M.A.; Brito, P.P.R.; Hadler, K.; Cole, K.; Cilliers, J.J. The effect of particle size distribution on froth stability in flotation. *Sep. Purif. Technol.* **2017**, *184*, 240–247. [[CrossRef](#)]
6. Tao, X.; Cao, Y.; Liu, J.; Shi, K.; Liu, J.; Fan, M. Studies on characteristics and flotation of a hard-to-float high-ash fine coal. In Proceedings of the 6th International Conference on Mining Science & Technology, Xuzhou, China, 18 October 2009.
7. Akdemir, Ü.; Sönmez, I. Investigation of coal and ash recovery and entrainment in flotation. *Fuel Process. Technol.* **2003**, *82*, 1–9. [[CrossRef](#)]
8. Li, C.; Xing, Y.; Gui, X.; Cao, Y. Enhancement of oxidized coal flotation by preconditioning with positive-charged microbubbles. *Int. J. Coal Prep. Util.* **2020**, *40*, 553–563. [[CrossRef](#)]
9. Zhang, Z.; Ren, L.; Zhang, Y. Role of nanobubbles in the flotation of fine rutile particles. *Miner. Eng.* **2021**, *172*, 107140. [[CrossRef](#)]
10. Huo, X.; Zuo, W.; Shi, F.; Huang, W. Coal middling retreatment using high voltage pulse technique. Part 1: Experimental findings. *Fuel* **2022**, *314*, 123066. [[CrossRef](#)]
11. Zhou, S.; Wang, X.; Bu, X.; Wang, M.; An, B.; Shao, H. A novel flotation technique combining carrier flotation and cavitation bubbles to enhance separation efficiency of ultra-fine particles. *Ultrason. Sonochem.* **2020**, *64*, 105005. [[CrossRef](#)]
12. Capes, C.E.; Darcovich, K. A survey of oil agglomeration in wet fine coal processing. *Powder Technol.* **1984**, *40*, 43–52. [[CrossRef](#)]
13. Kadagala, M.R.; Nikkam, S.; Tripathy, S.K. A review on flotation of coal using mixed reagent systems. *Miner. Eng.* **2021**, *173*, 107217. [[CrossRef](#)]
14. Dey, S. Enhancement in hydrophobicity of low rank coal by surfactants: A critical overview. *Fuel Process. Technol.* **2012**, *94*, 151–158. [[CrossRef](#)]
15. Vamvuka, D.; Agridiotis, V. The effect of chemical reagents on lignite flotation. *Int. J. Miner. Process.* **2001**, *61*, 209–224. [[CrossRef](#)]
16. Ozer, M.; Basha, O.M.; Morsi, B. Coal-Agglomeration Processes: A Review. *Int. J. Coal Prep. Util.* **2016**, *37*, 131–167. [[CrossRef](#)]
17. Chen, Y.; Zhou, B.; Zhang, X.; Yang, S.; Huang, W. Understanding the role of kerosene on the coal particle and bubble attachment process. *Fuel* **2022**, *307*, 121915. [[CrossRef](#)]
18. Zhao, J.; Fu, X.; Wang, J.; Song, G.; Wang, K. Influence of ultra-fine grinding mode on ultra-clean coal separation effect. *J. China Coal Soc.* **2016**, *41*, 3108–3114.
19. Xia, Y.; Zhang, R.; Xing, Y.; Gui, X. Improving the adsorption of oily collector on the surface of low-rank coal during flotation using a cationic surfactant: An experimental and molecular dynamics simulation study. *Fuel* **2019**, *235*, 687–695. [[CrossRef](#)]
20. Marsalek, R.; Pospisil, J.; Taraba, B. The influence of temperature on the adsorption of CTAB on coals. *Colloids Surf. A Physicochem. Eng. Asp.* **2011**, *383*, 80–85. [[CrossRef](#)]
21. Wen, B.; Xia, W.; Sokolovic, J.M. Recent advances in effective collectors for enhancing the flotation of low rank/oxidized coals. *Powder Technol.* **2017**, *319*, 1–11. [[CrossRef](#)]

22. Zou, W.; Gong, L.; Huang, J.; Zhang, Z.; Sun, C.; Zeng, H. Adsorption of hydrophobically modified polyacrylamide P(AM-NaAA-C(16)DMAAC) on model coal and clay surfaces and the effect on selective flocculation of fine coal. *Miner. Eng.* **2019**, *142*, 105887. [[CrossRef](#)]
23. Li, C.; Xu, M.; Zhang, H. Efficient separation of high-ash fine coal by the collaboration of nanobubbles and polyaluminum chloride. *Fuel* **2020**, *260*, 116325. [[CrossRef](#)]
24. Lv, S.; Peng, W.; Cao, Y.; Liu, S.; Wang, W.; Fan, G. Synthesis and characterisation of a novel pH-sensitive flocculant and its flocculation performance. *J. Mol. Liq.* **2022**, *348*, 118480. [[CrossRef](#)]
25. Palchoudhury, S.; Lead, J.R. A Facile and Cost-Effective Method for Separation of Oil-Water Mixtures Using Polymer-Coated Iron Oxide Nanoparticles. *Environ. Sci. Technol.* **2014**, *48*, 14558–14563. [[CrossRef](#)]
26. Alabresm, A.; Chen, Y.P.; Decho, A.W.; Lead, J. A novel method for the synergistic remediation of oil-water mixtures using nanoparticles and oil-degrading bacteria. *Sci. Total Environ.* **2018**, *630*, 1292–1297. [[CrossRef](#)] [[PubMed](#)]
27. Lin, Q.; Mei, Y.; Huang, W.; Zhang, B.; Liu, K. Understanding the Role of Polyvinylpyrrolidone on Ultrafine Low-Rank Coal Flotation. *ACS Omega* **2022**, *7*, 10196–10204. [[CrossRef](#)] [[PubMed](#)]
28. Barbian, N.; Ventura, M.E.; Cilliers, J.J. Dynamic froth stability in froth flotation. *Miner. Eng.* **2003**, *16*, 1111–1116. [[CrossRef](#)]
29. Bu, X.; Wang, X.; Zhou, S.; Li, B.; Zhan, H.; Xie, G. Discrimination of Six Flotation Kinetic Models Used in the Conventional Flotation and Carrier Flotation of  $-74\ \mu\text{m}$  Coal Fines. *ACS Omega* **2020**, *5*, 13813–13821. [[CrossRef](#)]
30. Xu, M. Modified flotation rate constant and selectivity index. *Miner. Eng.* **1998**, *11*, 271–278. [[CrossRef](#)]
31. Hu, S.; Chen, Y.; Wu, C.; Li, J.; Liu, K. The performance and dispersing mechanism of anionic dispersants in slurries prepared by upgraded coal. *Colloids Surf. A Physicochem. Eng. Asp.* **2020**, *606*, 125450. [[CrossRef](#)]
32. Zhang, Y.; Hu, S.; Yang, X.; Jiang, F.; Wu, C.; Li, J. Performance and mechanism of polyacrylamide stabilizers in coal water slurry. *Colloids Surf. A Physicochem. Eng. Asp.* **2021**, *630*, 127544. [[CrossRef](#)]
33. Li, L.; Li, Z.; Ma, C.; Wang, J.; Cao, X.; Wang, P. Molecular dynamics simulations of nonionic surfactant adsorbed on subbituminous coal model surface based on XPS analysis. *Mol. Simul.* **2019**, *45*, 736–742. [[CrossRef](#)]
34. Zhang, Q.; Niu, C.; Bu, X.; Bilal, M.; Ni, C.; Peng, Y. Enhancement of Flotation Performance of Oxidized Coal by the Mixture of Laurylamine Dipropylene Diamine and Kerosene. *Minerals* **2021**, *11*, 1271. [[CrossRef](#)]
35. Xing, Y.; Gui, X.; Karakas, F.; Cao, Y. Role of Collectors and Depressants in Mineral Flotation: A Theoretical Analysis Based on Extended DLVO Theory. *Minerals* **2017**, *7*, 223. [[CrossRef](#)]
36. Hussain, S.A.; Demirci, S.; Ozbayoglu, G. Zeta potential measurements on three clays from Turkey and effects of clays on coal flotation. *J. Colloid Interface Sci.* **1996**, *184*, 535–541. [[CrossRef](#)]
37. Sahoo, H.; Sinha, N.; Rath, S.S.; Das, B. Ionic liquids as novel quartz collectors: Insights from experiments and theory. *Chem. Eng. J.* **2015**, *273*, 46–54. [[CrossRef](#)]
38. Tian, M.; Khoso, S.A.; Wang, L.; Sun, W.; Zhang, C.; Hu, Y. Selective separation behavior and its molecular mechanism of cassiterite from quartz using cupferron as a novel flotation collector with a lower dosage of  $\text{Pb}^{2+}$  ions. *Appl. Surf. Sci.* **2019**, *486*, 228–238. [[CrossRef](#)]